İSTANBUL UNIVERSITY CERRAHPAŞA

REVIEW
Electrica 2023; 23(3): 681-694

Performance and Comparison of Voltage Compensation Based on Hybrid Metaheuristic Technique Tuned Z-Dynamic Voltage Restorer

Ch Srivardhan Kumar, Z Mary Livinsa

Sathyabama Institute of Science and Technology, Chennai, India

Cite this article as: C.S. Kumar and Z.M. Livinsa, "Performance and comparison of voltage compensation based on hybrid metaheuristic technique tuned Z-dynamic voltage restorer," *Electrica*, 23(3), 681-694, 2023.

ABSTRACT

The main cause for concern is power quality (PQ) problems, specifically voltage disturbances, fluctuation, sag, harmonics, and swell in the power distribution system. To correct these voltage disturbances in the electrical power distribution system, an efficient device called a dynamic voltage restorer (DVR) is integrated between the source and the load. In this study, DVR is integrated with the source to protect the sensitive load from voltage disturbances caused by the source side under non-linear load conditions. In addition, a unique Z-type source inverter (ZSI) is introduced to improve the restoration of the voltage property of DVR. This ZSI ensures that the direct current (DC) link used for the compensation process maintains a constant DC voltage. By adjusting the gain parameters of the proportional–integral–derivative (PID) controller and accounting for voltage problems such as sag, fluctuation, swell, and interruption in the load side, the hybrid Harris hawks optimization (HHO) and black widow optimization (BWO) are also utilized to regulate the Z-source DVR (Z-DVR). The 2020Ra version of MATLAB/Simulink is used to implement this proposed work and analyze the outcomes. HHO–BWO is also compared to earlier works like BWO–PID, HHO–PID, genetic algorithm–PID, and mm-sized resistance-typed sensor film controller to demonstrate its superiority in terms of total harmonic distribution and problem-solving.

***Index Terms*—**Direct current link voltage, gain parameters, non-linear load, proportional–integral–derivative controller, voltage issues

I. INTRODUCTION

Controlling power quality (PQ) is important in contemporary distribution power systems since voltage problems like harmonics, sag, and swell can cause transient as well as steady-state concerns. Sensitive loads may experience severe disruptions as a result of this significant loss of production, even though communication networks, home, medical, and even office automation are now widely used in the industry. To operate continuously for 24 hours, it needs an unstable input power supply, highly stable input, and power [1–3]. Additionally, a fault developed in the integrated power system as a result of the effect of input power disturbances, specifically voltage sags or interruptions. The ground fault that results in a significant drop in the voltage bus's distribution lines has an impact on the load performance as well. Then, by adding zero sequence and negative voltages, many PQ issues are brought on by unbalanced three-phase loads, and there is also a probability that voltage swells may occur in the grid when there are low loads [4, 5]. By integrating the non-linear loads that introduce harmonics into the distribution system, the system's power loss is exacerbated. As a result, it is critical to maintain PQ issues for technological requirements to supply power to sensitive loads [6].

The flexible alternating current transmission systems (FACTS) devices, active filters, unified power quality conditioner, dynamic voltage restorer (DVR), and distribution static compensator were used to develop several significant techniques to improve PQ in the power system. PQ problems can be fixed by integrating these devices either parallelly or serially. The shunt, integrated shunt-series, and series devices are used for PQ reimbursement. The use of unified power flow controller for compensating voltage and current was common. A current compensator is integrated into the shunt with the common point of connection [7–10]. The first adaptable gadget is DVR, which can be used to correct voltage-related issues. Until now, DVR has been used to reduce the impact of voltage sag because it has been widely used in dynamic positioning system for series compensation and is a cost-accurate device. To improve the DVR's dynamic behavior, control strategies, topologies, and range of operation have been expanded. DVR is used in series compensation to

Corresponding author:
Ch Srivardhan Kumar

E-mail:
Srivardhankumar4813@gmail.com

Received: December 22, 2022

Accepted: May 15, 2023

Publication Date: July 20, 2023

DOI: 10.5152/electr.2023.22229

reduce swell and sag. By using DVR, voltage harmonics and variations can be effectively reduced. Additionally, it can buck or boost the voltage on the alternating current (AC) bus by compensating the device serially, protecting sensitive loads from voltage variations. Voltage swell, sag, and harmonics are often occurring power problems in the power system [11–13].

Sag voltage is the phrase for the abrupt occurrence of short voltage and the impulsive lowering of root mean square voltage caused by the excess load. Voltage swell occurs when an overload is abruptly shut off because of an increase in system voltage. Voltage/current harmonics are defined as the unwanted multiples of current and voltage in the power system [14, 15]. In this study, the Z-DVR is controlled by a proportional–integral–derivative (PID) controller-based hybrid optimized technique called black widow optimization–Harris hawks optimization (BWO–HHO), and the series compensating device is used to improve voltage quality. Constraints taken into account for Z-DVR faulty controller include minimizing active power exchanged and the potential for voltage injection.

II. LITERATURE REVIEW

Many researchers have presented a variety of solutions to address the voltage issues caused by the integration of FACTS devices.

Al-Ammar et al. [16] used a flexible control-based synchronous reference frame theory approach with DVR in the distribution system to reduce voltage sag. The DVR was connected in series with the load bus through the combination of a filter and an injection transformer. The proposed approach with DVR was superior at reducing voltage sag. The author failed to build the DVR's control structure on sliding mode control and fuzzy logic control.

Joshi et al. [17] improved voltage stability in the transmission system by controlling the reactive power flow with a static Volt-Amps Reactive (VAR) compensator (SVC). The ideal number of SVCs for reactive power control needed to be automatically determined. The voltage stability was improved with the help of the suggested strategy.

Moreno et al. [18] presented an evaluation and implementation of a modified DVR with AC link for series compensation. The AC voltage was corrected using DVR assisted by transformer (AT-DVR) to reduce swelling and sagging. The effectiveness of AT-DVR for compensating asymmetrical events was immediately assessed. Using a streamlined control modulation vector approach, swell and sag asymmetrical events were reduced.

Bhonde et al. [19] increased the quality of the electricity by series compensating while using DVR in the power system. To correct for both voltage swell and sag, a DVR based on sine vector template generation was used. DVR also offered excellent voltage regulation, quickly resolving voltage-related concerns. Both unbalanced and balanced conditions can be immediately corrected by the DVR by correctly injecting the voltage component.

Ray et al. [20] have developed a custom power device based on a fuzzy controller in a photovoltaic (PV) system to improve PQ. A 3-φ shunt hybrid active filter combined with PV and a direct current (DC)/DC boost converter was used to compensate for voltage harmonics, swell, and sag due to the non-linear power electronic demand. Comparing the analysis to other traditional methods, it was accurate in compensating for harmonics. The maximum power point tracking was created with the grid DC/AC inverter as the restriction to achieve enhancement in reactive power and PQ mitigation.

The improvement of sag voltage used with DVR and hybrid renewable energy systems (HRES) combined with sensitive loads has been presented by Molla and Kuo [21]. The system became unstable due to fault situations or unstable output power from the HRES, which caused voltage fluctuations that were reduced by the DVR and the protection of the vulnerable loads. The swell, harmonics, and fluctuation of the voltage signal are not examined by the author.

The DVR was introduced by Rajasekaran et al. [22] to reduce voltage sag and swell with great dependability and rapid reaction. This method effectively reduces the problems caused by voltage sag and swell in the power supply. Additionally, DVR manages the unbalanced and balanced loads and successfully keeps the system in a balanced state.

To address the voltage sag and swell issues in the grid system, Babaei et al. [23] have presented the DVR based on the PV system. The sag and swell signal generated by the PV that is integrated with the grid-connected system was also studied in this work to improve system dependability. Because the DVR was dependent on the phase shift angle, which is dependent on the battery's ability to charge and discharge, it could not be controlled directly.

The proton exchange membrane fuel cell (PEMF) is one type of fuel cell DVR with PID controller and Fuzzy Logic (FL) technique optimized with genetic algorithm (GA) has been presented by Sundarabalan and Selvi [24] to mitigate voltage swell, sag, and harmonics as well as total harmonic distribution (THD) value reduction. The comparison that was made between only the medium voltage level DVR and not with other low voltage and high voltage level DVR is not properly analyzed by the author.

To control the stability of the voltage in the distribution system, Ingole and Gohokar [25] presented the static synchronous series compensator integrated with IEEE 9 bus system. This control method is being used in this project to regulate the voltage and maintain a steady stream of power. The author does not examine the power system's voltage problems.

An active power filter has been used to mitigate the sag and swell [26]. The proposed method was verified using MATLAB/SIMULINK. The repetitive controller with third harmonic injection technique is applied to achieve better dc-link utilization for medium–low voltage distribution [27]. As an outcome, it is indeed evident that 15% reflects an increment in dc bus utilization as well as the potential to create high voltage. A PV-integrated DVR using a rotating dq reference frame controller with an optimum tuned PID controller has been proposed in [28].

However, the bulk of voltage issues in the prior research was recognized and reduced by using appropriate techniques for adjusting voltage quality. Thus, a unique control methodology based on optimized hybrid HHO–BWO-based Z-DVR with PID controller will develop on the grid-integrated system to compensate for voltage quality issues, that is, voltage swell, sag, harmonics, interruptions, and fluctuation. The grid-integrated system will therefore require a design with a special control approach based on an improved hybrid HHO–BWO-based Z-DVR with PID controller to correct voltage quality concerns, such as voltage swell, sag, harmonics, interruptions, and fluctuation.

III. PROPOSED CONTROL SCHEME FOR PQ

Clients suffer direct or indirect financial losses as a result of PQ issues that occur from lost manufacturing production, equipment damage, intrusion procedures, material waste, and data problems. In practice, even small voltage sags can disrupt the process for a few hours, and PQ problems can impair security systems as well as measurement equipment like dispatchers and breakers. These problems also interfered with business operations and checking systems. Z-type source inverter (ZSI)-based DVR is the best choice to increase PQ and enhance the system if a voltage issue in the power supply arises. The yield of the compensators is determined by the circuit's controlled process. Therefore, a variety of ideologies are suggested to give enhanced power differentiation of the power structure. On the other hand, the PQ falls short of the cover. In some cases, using AI to improve the DVR's execution and determine the appropriate regulating strategy for this function may make the distributed power system's PQ problems worse. The overall architecture of the proposed methodology is illustrated in Fig. 1.

A. Issues Occurred in PQ

PQ problems are the distribution system's main significant challenge. It almost exclusively happens as a result of load differences and random fluctuations. Voltage sag/swell/fluctuation and interruption are the most significant PQ issues in the distributed system, occurring more frequently than a range of other PQ issues. Following is a brief discussion of the previously mentioned PQ issues:

1) Formation of Sag Voltage

In the distribution system, the sag voltage is a frequent and harmful PQ problem when it comes to sensitive loads in dangerous situations. Short circuits and overload connections are two of the most frequent reasons for sagging voltages. When a ground fault occurs on the feeder system, the majority of the sag voltage manifests itself. The nominal voltage level decreases as various exchanging operations characterize the relative change, such as a wise voltage list. The relative voltage adjustment shown in (1) is as follows:

$$\Delta V_{sag}^{*} = k^{*} \frac{p_{RA}^{*}}{p_{SCA}^{*}} \tag{1}$$

k^{*} = Factor of voltage reduction,

p_{RA}^{*} = Apparent power rate,

p_{SCA}^{*} = Apparent power of short-circuit.

However, the range where sag voltage occurs is less than or equal to 3%.

2) Formation of Swell Voltage

The swell voltage occurs on the dispersed system as a result of the single line-to-ground error; additionally, a brief voltage rise may occasionally occur in the fault-free stages. As a function of maximum apparent power p_{max}^{*}, the rise of the voltage ΔV_{swell}^{*} can be evaluated at the point of common coupling (PCC).

$$\Delta V_{swell}^{*} = \frac{p_{max}^{*}\left(z_{a}^{*}\cos\delta - z_{b}^{*}\sin\delta\right)}{v_{*}^{2}} \tag{2}$$

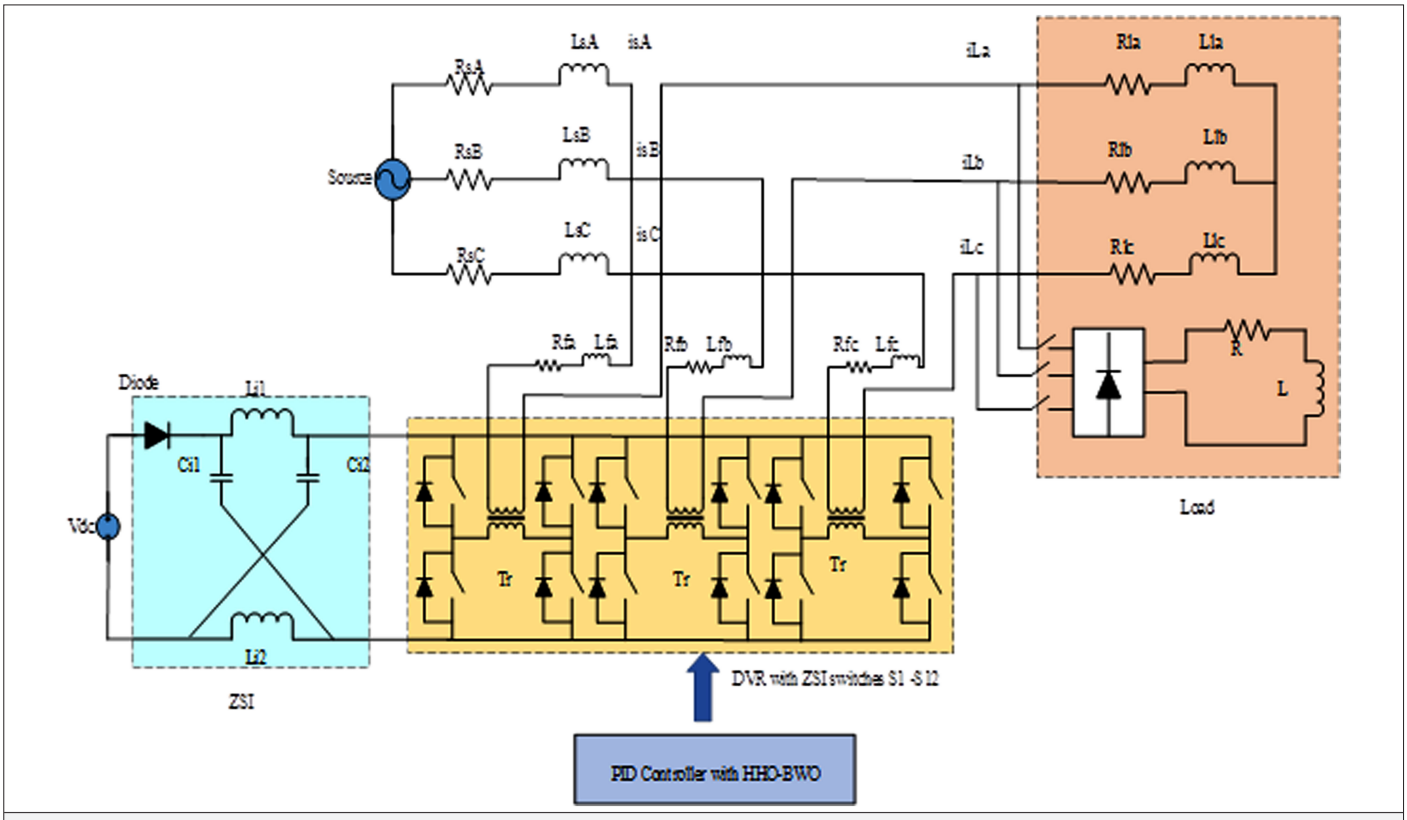

Fig. 1. Configuration of proposed Z-DVR. Z-DVR, Z-source dynamic voltage restorer.

δ = Phase angle,

z_a^* and z_b^* = Impedances of the grid.

However, the rise in voltage is nearly 2%.

3) Formation of Fluctuation

Signal-modulated oscillation of voltage value and amplitude at a frequency of 0 to 30 Hz. Because of the differences in output power, voltage fluctuation might happen. This depends on the generator's characteristics, the source's kind, and the network's impedance. As per the emission limits guidelines, fluctuation can be estimated for fluctuating loads in the high and medium voltage networks and for most countries, $\mp$ 10% variation is allowed.

$$I^* = \frac{p^* - jq^*}{U_{pcc}^*} \tag{3}$$

I^* = Line current,

p^* = Output real power in DG system,

q^* = Output reactive power in DG system,

U_{pcc}^* = Voltage at PCC.

4) Formation of Interruption

Some standards refer to discontinuities as interruptions to a consumer supply. There are two types of interruptions: short-term interruptions and long-term interruptions. This essay examines brief interruptions that last no more than 1 minute.

5) Harmonics

When a sensitive load is present, the voltage degrades, which causes harmonic distortion. The decrease in harmonics maintains a limited amount of harmonic voltage. Concerning the voltage, the THD is given in (4),

$$V_{THD}^* = \sqrt{\sum_{N=2}^{\infty} \frac{V_N^2}{f_j^*}} \times 100\% \tag{4}$$

V_N = n-th harmonic voltage,

f_j^* = Fundamental frequency,

However, the THD value is attained at 3%.

To address voltage issues with the DG system, such as sag, fluctuation, swell, harmonics, and interruption, the appropriate and effective device must be added at PCC. The suggested system combines a hybrid HHO–BWO control strategy with a ZSI-DVR.

The ZSI network, which is coupled at the DC link side, is an impedance network that uses a lattice structure. The ZSI is preferable to the traditional converter because of its buck and boost properties. The system reliability is increased as a result of the ZSI's immunity to EMI noise. Because ZSI works as a second-order filter, it requires inductance and capacitance with reduced values. Small amounts of inductance and capacitance across the inverter produce a steady DC link voltage. Additionally, it has three different settings, including shot through, active, and zero.

$$c_1^* = c_2^* = c^* \tag{5}$$

$$L_1^* = L_2^* = L^* \tag{6}$$

From the abovementioned condition,

$$I_{L1}^* = I_{L2}^* = I_L^* \tag{7}$$

$$I_{C1}^* = I_{C2}^* = I_C^* \tag{8}$$

The input voltage of the inverter is given by,

$$V_I^* = \beta^* V_{DC}^* \tag{9}$$

V_{DC}^* = DC link voltage,

β^* = Boosting factor.

$$\beta^* = \frac{1}{1 - 2\left(\frac{t_0}{t}\right)} \tag{10}$$

t_0 = In shoot through mode, time period,

t = Switching time.

B. Working Modes of DVR Controller

The primary function of the DVR is to inject dynamically regulated voltage into the transport voltage as well as voltage produced by a limited commutated converter using the booster transformer. To prevent any detrimental consequences of a bus failure on the voltage of the load, for instance, the three infused stage voltages, which are transitory amplitudes, are regulated. It has three modes:

1. Protection mode.
2. Standby mode or zero mode.
3. Boost mode or injection mode.

1) Protection Mode

If the load-side current rises above a tolerable limit due to a load-side short-circuit or a large inrush current, the DVR will be separated from the system by using the bypass switches (S_2^* and S_3^*) to provide an alternative path for the current (S_1^* will be closed).

2) Standby Mode or Zero Mode

When the DVR voltage is zero and in zero modes, the converter lowers the minor voltage winding of the booster transformer. Since no semiconductor exchange is happening, the full load current will flow through the primary winding in this functional mode.

3) Boost Mode or Injection Mode

While in boost or injection mode, DVR will inject a compensating voltage with the aid of the transformer as soon as it notices variations in the source voltage. The DVR will therefore be utilized in injection mode for this project.

C. Strategies for Compensation

Following is a demonstration of the four different techniques of voltage injection of DVR depending on several limiting criteria, such as types of voltage issues, load situations, and DVR power rating, when the injection mode DVR is employed.

1) Pre-Dip/Sag Compensation Technique

In this type, the load voltage's magnitude and phase angle are returned to their pre-sag values and phase leaps can also be adjusted. However, more active power from the DC link capacitor is required for this phase leap rectification. Because of the greater phase angle between the load current and the source voltage during the positive phase leap compared to the negative phase jump, the DVR's performance reduced and increased in active power. In some criteria, the DVR inserted the magnitude and phase angle of the voltage that is illustrated in the later equations:

$$V_{dvr}^{*}=\sqrt{2\left(V_{L}^{*2}+V_{S}^{*2}\right)-2V_{L}^{*}V_{S}^{*'}\cos\left(\delta\right)} \tag{11}$$

$$\angle V_{dvr}^{*}=\tan^{-1}\left(\frac{V_{L}^{*}\sin\theta_{L}^{*}-V_{S}^{*'}\sin\left(\theta_{L}^{*}-\delta\right)}{V_{S}^{*'}\cos\left(\theta_{L}^{*}-\delta\right)-V_{L}^{*}\cos\theta_{L}^{*}}\right) \tag{12}$$

δ = Due to sag condition, phase jump in grid voltage,

$V_{L}^{'*}$ = Before sag, load voltage,

$V_{S}^{*'}$ = Sag supply voltage.

2) In-Phase Compensation Method

This approach cannot eliminate the phase jump due to the sagging supply voltage due to the small amount of feasible magnitude and phase of the voltage injection by the DVR. The injected voltage magnitude and phase of DVR equations are illustrated in the equations, respectively,

$$V_{dvr}^{*}=V_{1}^{*}=\sqrt{2}(V_{L}^{*}-V_{S}^{*'}) \tag{13}$$

$$\angle V_{dvr}^{*}=\theta_{L}^{*} \tag{14}$$

3) Method of Energy Optimization

This kind of reimbursement is designed for sag depths more profound than the restraint to enhance the performance of the quadrature injection technique. The DVR injects a certain amount of active power, and the voltage magnitude and injection angle of the DVR equations are shown later,

$$V_{dvr}^{*}=\sqrt{2\left(V_{L}^{*2}+V_{S}^{*2}\right)-2V_{L}^{*}V_{S}^{*'}\cos\left(\theta_{L}^{*}\right)} \tag{15}$$

$$\angle V_{dvr}^{*}=\tan^{-1}\left(\frac{V_{L}^{*}\sin\theta_{L}^{*}}{V_{L}^{*'}\cos\left(\theta_{L}^{*}\right)-V_{S}^{*}\cos\theta_{L}^{*}}\right) \tag{16}$$

The choice of one of these plans affects the DVR strategy and parameters. The acceptable regulator strategy in this study to maintain load voltage at pre-fault levels is pre-sag reimbursement.

IV. CONTROL TECHNIQUES OF THE PROPOSED METHOD

A. Hybrid HHO and WOA Algorithms

The suggested study integrates metaheuristic-based HHO and BWO algorithms to adjust the gain parameters of the PID controller. The following section provided distinct descriptions of the HHO and BWO optimization methods.

1) HHO Algorithm

The cooperative chasing behavior of Harris hawks serves as the foundation for the HHO algorithm. Numerous scientific applications of the HHO technique have proved successful. The hawks startle their victim (a rabbit) by pouncing on it in various ways. Based on the flight patterns of their prey, Harris hawks choose the style of pursuit. The three stages of HHO are pounce, track, and attack.

The waiting, looking for, and discovery of the desired chase are also part of the exploration phase. The second step of the HHO is the shift from exploration to exploitation, and the third stage is the exploitation phase, which is predicated on the prey's remaining energy. Hawks pursue rabbits from a variety of angles using two forms of besieging, SB and HB, with SB being the more frequent and HB being the less frequent.

Exploration, transformation, and exploitation are the three stages of HHO. Throughout the exploring phase, hawks randomly discovered new locations to watch and catch a rabbit. Hawks benefit from the presence of nearby hawks when they are investigating. The hawks' stance is thought of as a potential response. The ideal situation for a rabbit is one that he should be in. The following are three phases to be aware of:

a) Exploration phase

This phase involves the waiting, searching, and detecting of prey. The following is a representation of a hawk's position:

$$n_{j}\left(V+1\right)=\begin{cases}n_{j_{rand}}\left(\mathrm{V}\right)-\gamma_{1}\left|n_{j_{rand}}\left(\mathrm{V}\right)-2n_{j}\gamma_{2}\right.\\ \left(V\right)\left|\,if\,m\geq 0.5\right.\\ n_{j_{q}}\left(V\right)n_{j_{a}}\left(V\right)-\gamma_{3}(l_{1}+\gamma_{4}\\ \left(v_{b}-l_{1}\right))if\,m<0.5\end{cases} \tag{17}$$

The present iteration is represented as V, and the next iteration represents as $V+1$. The location of the hawks is represented as γ_1, γ_2, γ_3, and γ_4, while the range of [0, 1] expressed the random number y. The hawk's average location n_{j_a} is expressed as

$$n_{j}\left(V+1\right)=\Delta n_{ja}\left(V\right)=\frac{1}{N}\sum_{i=1}^{N}n_{j}\left(V\right) \tag{18}$$

b) Transformation phase

The exploitation phase sees a shift from the discovery phase. Prey energy was broken down as the prey was evading. It was defined as,

$$\omega_{prey}=2\omega_{0}\left(1-\frac{V}{V_{max}}\right) \tag{19}$$

where the prey's initial energy state is ω_0, the present number iteration is denoted as V and the maximum iteration number is represented as V_{max}.

c) Exploitation phase

The hawk's attack on the selected prey in the initial phase is used to assess it. The four different strategies that were taken into consideration in this phase were SB, HB, SB with progressive fast dives, and HB with progressive fast dives. On the energy level, the occurrence of hard and soft relies was $\left|\omega_{prey}\right|\geq 0.5$ and $\left|\omega_{prey}\right|<0.5$.

d) Besiege for soft
SB method can be selected, if $|\omega_{prey}| \geq 0.5$ and $\gamma \geq 0.5$. It is defined as:

$$n_j(V+1) = \Delta n_j(V) - \omega_{prey} \left| \zeta n_j(V - n_j(V)) \right| \quad (20)$$

Here, eluding process for jump intensity is ζ which is determined by $\zeta = 2(1-\gamma_5)$ and $= \Delta n_j(V) = n_{prey}(V) - n_j(V)$.

e) Besiege for hard
HB can be selected, if ≥ 0.5 and $|\omega_{prey}| < 0.5$. It is defined as:

$$n_j(V+1) = n_{prey}(V) - \omega_{prey} \left| \Delta n_j(V) \right| \quad (21)$$

f) Besiege for soft With high progressive dives
SB method can be selected, if $\gamma < 0.5$ and $|\omega_{prey}| \geq 0.5$. It is determined as:

$$\varrho = n_j(M) - \omega_{prey} \left| \zeta n_{prey}(V - n_j(V)) \right| \quad (22)$$

The hawk's next moving step (ϱ) is computed next. Further, the following equation is expressed to attack the prey when hawks dive,

$$D_n = \varrho + R * LF(d) \quad (23)$$

where the random vector is expressed as R as well as the dimension d of levy flight is defined as $LF(d)$. The updated location is determined as,

$$n_j(V+1) = \begin{cases} \varrho \, if \, f(\varrho) < f(n_j(V)) \\ D_n \, if \, f(D_n) < f(n_j(V)) \end{cases} \quad (24)$$

g) Besiege for hard With high progressive dives
SB method has been selected, if $\gamma < 0.5$ and $|\omega_{prey}| < 0.5$. It is determined by the updated location:

$$n_j(V+1) = \begin{cases} \varrho \, if \, f(\varrho) < f(n_j(V)) \\ D_n \, if \, f(D_n) < f(n_j(V)) \end{cases} \quad (25)$$

From, the following equation is determined by ϱ ,

$$\varrho = y_{prey}(V) - \omega_{prey} \left| \zeta n_{prey}(V - n_{ja}(V)) \right| \quad (26)$$

Based on the HHO technique, the population's fitness-based location of prey is updated.

2) Black Widow Optimization
The BWO strategy is based on the lifecycle of the black widow spider. The female black widow spider spends the day hiding, and then at night, they spin their webs. Majority of her adult life she spends in the same place. She employs a pheromone to entice the male spider to particular sections of her web and attracts the male spider for mating. After mating, the female spider eats her mating partner before transferring the eggs to the egg sock. Once the eggs hatch, sibling cannibalism ensues. However, they do spend a limited period on their mother's web, and they may even consume the mother spider, which helps the fit and strong survive.

The first is known as sexual cannibalism, where female spiders eat male spiders either during or after mating. This method can be used to determine the fitness value of populations of male and female spiders. The second type is sibling cannibalism, where strong young spiders eat weaker young spiders. This theory ensures that only the fittest young spiders remain in the colony, expelling the others. In the third type, young spiders eat their mothers. This concept practices the fitness values of the mother and the young spiders.

3) Mathematical Evaluation of Cannibalism Process in Sibling
Black widow populations are chosen at random to start the BWO method. This random population includes both male and female black widows for the following generation. The following is the original population of the black widow:

$$X_{N,d} = \left[x_{1,1} \, x_{1,2} \, x_{1,3} \ldots\ldots x_{1,d} \right] \quad (27)$$

where $X_{N,d}$ is the population of the black widow, *d* is the number of decision variables, *N* is the population number, and *ub* is the upper bound of the population.

The potential solution population ($X_{N,d}$) is used to minimize or maximize the objective function and it is expressed as follows:

$$Objective\,Function = f(X_{N,d}) \quad (28)$$

In the proposed BWO model, various predefined parameters are specified such as Q_{pt} , Q_e , R_P,R_E, Ω_{ts} , Ω_{es} , Ω_{er} , and Ω_{sr} which are defined in the previous sections. These parameters are used to indicate the upper and lower bounds of P_e and P_s .

The upper bound of P_e is $P_{e\,max}$, lower bound of P_e is $\frac{Q_E - P_{pt}\Omega_{ts}}{\Omega_{es}}$, upper bound of P_s is $\frac{Q_P - P_{e.max}\Omega_{er}}{\Omega_{es}}$, upper bound of P_s is $\frac{Q_P - \left(Q_E - P_{pt}\Omega_{ts}\right)\Omega_{er} / \Omega_{es}}{\Omega_{sr}}$, and the lower bound of P_s is $\frac{Q_P - P_{e.max}\Omega_{er}}{\Omega_{sr}}$,

The next stage of black widow optimization is mutation. When choosing juvenile spiders, the mutation rate is considered. A young spider is chosen and given a small random value to undergo mutation.

$$Z_{k,d} = ¥_{k,d} + \alpha \quad (29)$$

where $Z_{k,d}$ is the mutated population of black widows, $¥_{k,d}$ is the randomly selected young spider, *k* is the randomly selected number, and α is the random mutate value.

Figure 2 shows the HHO–BWO flowchart for the proposed work. The parameters of the HHO are initialized and include the population of the HHO algorithm as well as the voltage and current that are driven from the grid. Following that, fitness calculations and updates are made. Before starting exploration or exploitation, ascertain the energy situation, and adjust the gain value of the PID controller. Next, check the iteration condition. Update the best gain values if the maximum iteration has been reached; otherwise, rerun the HHO fitness computation. Additionally, the initialization of the BWO algorithms is carried out to obtain a more optimal result. The PID controller's gain parameters are then adjusted and provided to it using the BWO technique.

B. PID Controller With Hybrid Optimization Technique
By integrating the relay feature approach with clever algorithms based on the PID self-setting theory, such as neural mesh, fuzzy

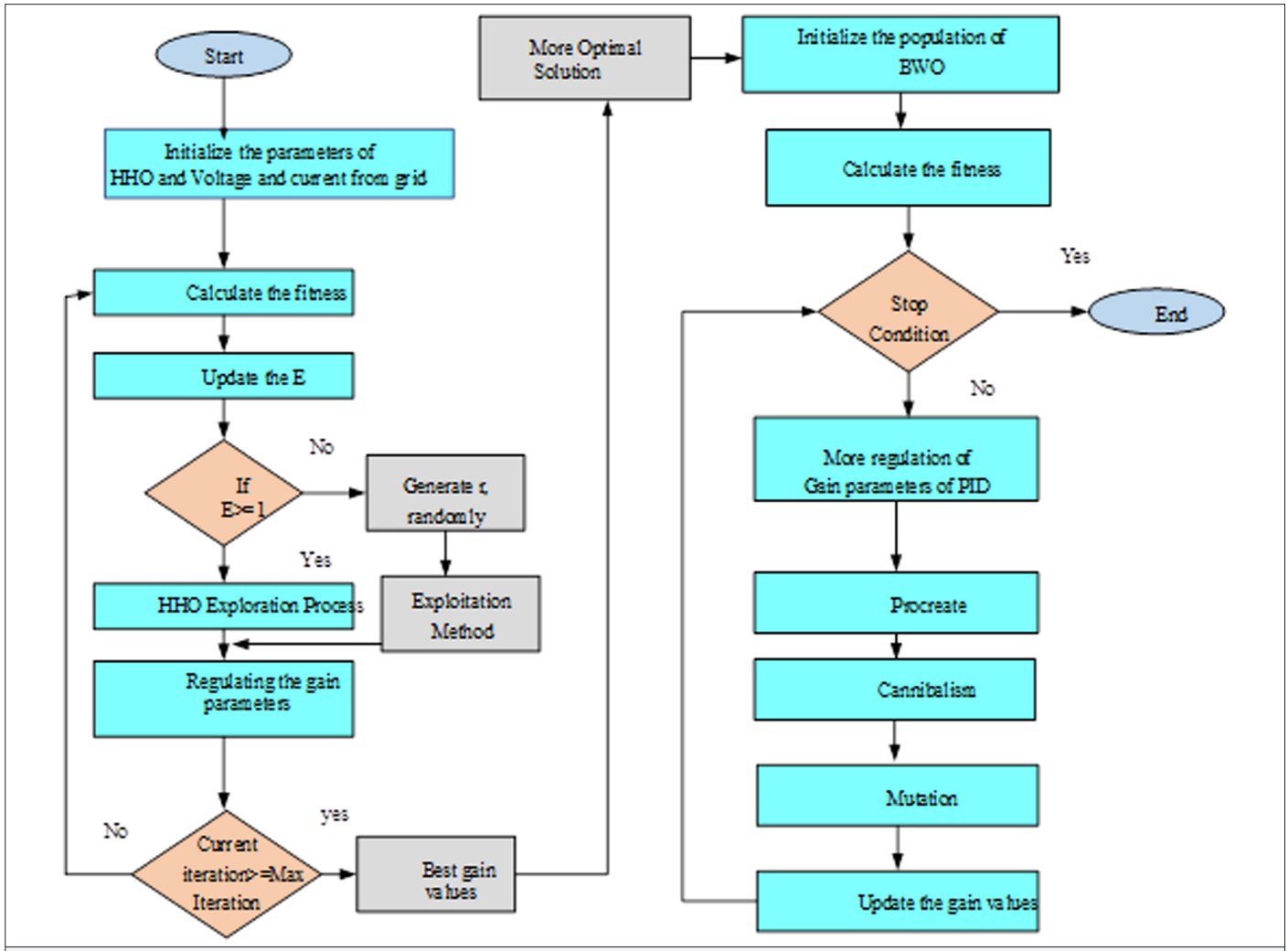

Fig. 2. Flowchart of the hybrid HHO–BWO. BWO, black widow optimization; HHO, Harris hawks optimization.

control, and adaptive gain (AG), several researchers also offered several updated techniques to increase the controller control impact. However, as time went on, the algorithm grew more complex and the setting speed was constrained, which was completely at odds with the simple PID controller's initial intent. Another study improved the system's control effect during actual operation by combining the hybrid HHO–BWO algorithm with self-specification, but actual HHO–BWO implementation would be more costly and time-consuming. Fig. 3 demonstrates a rapid and efficient method for fine-tuning the PID device parameter.

Finally, these revised settings are sent to the PID controller, and gate pulses are sent to the Z-DVR switches.

V. SIMULATION RESULTS AND MODELLING ANALYSIS

The implementation of Z-DVR with hybrid HHO–BWO has been established in this study as a means of addressing PQ concerns. This work is designed with the Z-DVR, and Table I contains Simulink's settings.

Figure 4 demonstrates the proposed Simulink structure with 3-φ power system which has 50 Hz frequency and 380 V implemented together with Z-DVR. In Fig. 4, the Z-DVR is serially integrated between the PCC and the non-linear sensitive load with the aid of the injection transformer. The Z-DVR also uses the injection transformer to inject the controlled voltage into the grid, which is the fundamental objective of the Z-DVR. The proposed work is built using MATLAB/Simulink 2020-Ra and Windows 10 PRO, with a total

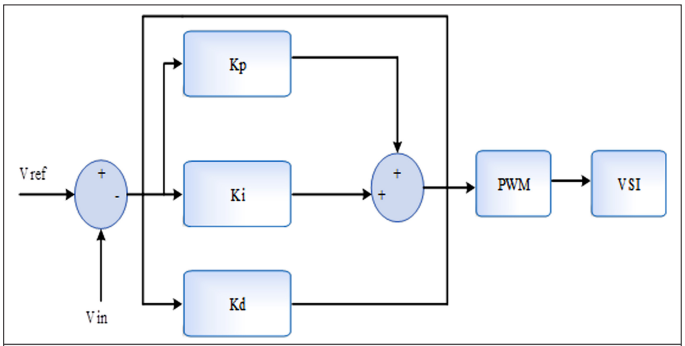

Fig. 3. PID controller. PID, proportional–integral–derivative controller.

TABLE I. PARAMETERS FOR SIMULINK

S. No	Block Name	Parameters	Values
1	Grid	Frequency	50 Hz
		Generator type	Swing
		Phase	0
2	Series	Resistance	1 Ω
		Capacitance	100 μF
3	Filter	Resistance	0.4 Ω
		Inductance	15 mH
4	Load	Resistance	60 Ω
		Inductance	0.15 mH
5	DC supply	Voltage	700 V
6	Z-DVR	Inductance	1000 mH
		Capacitance	2000 μF
7	Transformer	Nominal power	4000 VA
		Frequency	50 Hz

DC, direct current; Z-DVR, Z-source dynamic voltage restorer.

memory capacity of 8 GB and an Intel ® core (TM) i3-6098P CPU running at 3.60 GHz as the processor.

A graphical illustration of the suggested simulation is shown in Fig. 5. Three defects are computed and evaluated in the suggested technique. The proposed method is applied to identify voltage problems such as swell, fluctuation, sag, interruptions, and THD. In the simulation figure, a 3-φ is used as an input source, and a 3-φ-transformer is used to step up and down the voltage and current. The Z-DVR is used to correct voltage quality concerns between the source and the 3-φ parallel Resistor Indictor Capacitor (RLC) loads. To create faults including voltage swell, fluctuation, sag, interruption, and harmonics as well as a breaker to protect the circuit/system from hazardous conditions, a faulted device is connected to the source side.

The Z-DVR is employed to correct for voltage and satisfy load demand to avoid voltage issues. In this section, the implementation is carried out using the appropriate control mechanism employing a ZSI-based DVR. Under RLC load conditions, a Z-DVR with an improved HHO-BWO controller is suggested for adjusting voltage sag and fluctuation. To control the RLC load connection on the distribution system, a 3-φ breaker is used. Because of the quick change in heavy load, the source voltage sags as well as fluctuates. To compensate for the PQ issues in the distribution system, the hybrid HHO–BWO control structure is applied with Z-DVR (Fig. 6).

Figure 7 shows how a 3-φ fault is applied between 0.06 and 0.12 seconds for sag, 0.15 and 0.25 seconds for the interruption, and 0.35 and 0.42 seconds for the swell in the supply to see how the Z-DVR for voltage compensation is implemented. This also shows a very little amount of the voltage harmonics signal that the Z-DVR produced as it injected voltage into the load voltage. The filter's harmonic voltage drop is what causes this injected voltage to happen. Additionally, it explains the root mean square (RMS) of the source signal with the identical period fault and corrected load voltage. Here, 20% of sag is initiated from 0.06 seconds and kept until 0.12 seconds, voltage interruption is started from 0.15 seconds to 0.25 seconds, and voltage swell is created from 0.35 seconds to 0.42 seconds. The Z-DVR model was regulated by the proposed HHO–BWO to account for the severity of the voltage problems.

Then, to analyze the implementation of the Z-DVR for voltage compensation, the 3-φ fault is applied between the time durations of 0.06 seconds to 0.12 seconds for sag with fluctuating signal, 0.15 seconds to 0.25 seconds for interruption with fluctuating signal, and 0.35 seconds to 0.42 seconds for swell with fluctuating signal in the

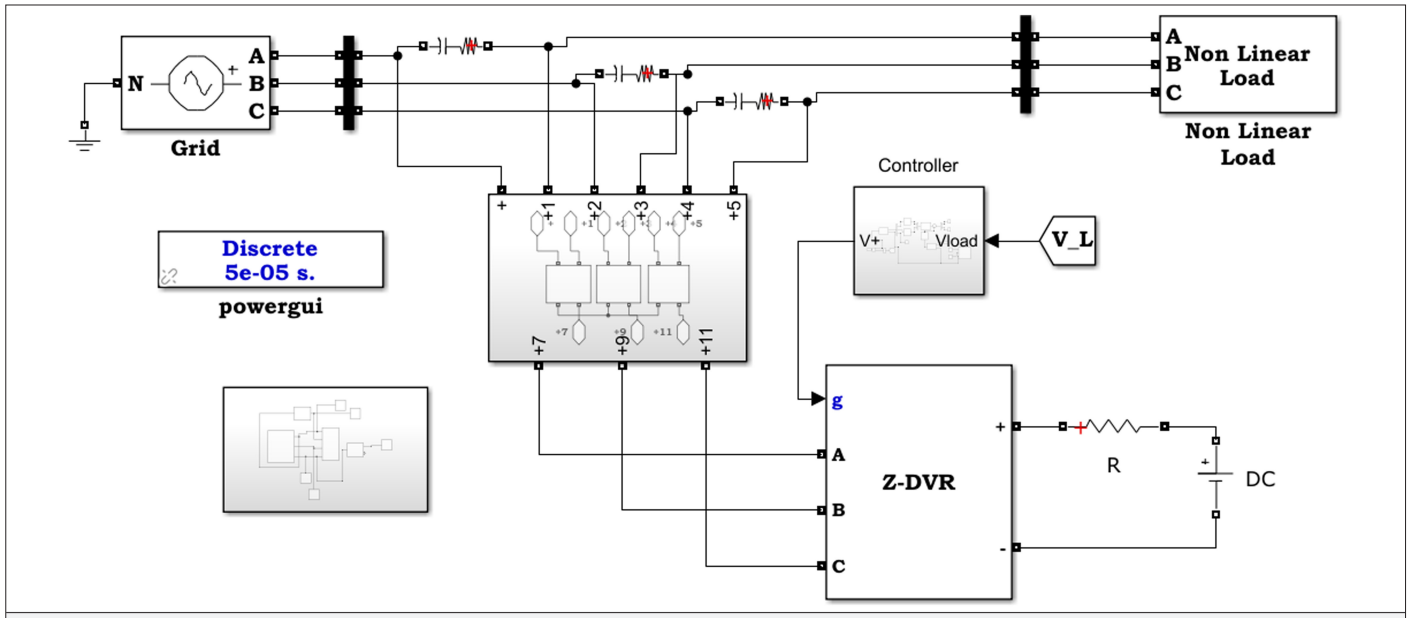

Fig. 4. Comparison of the swell compensation.

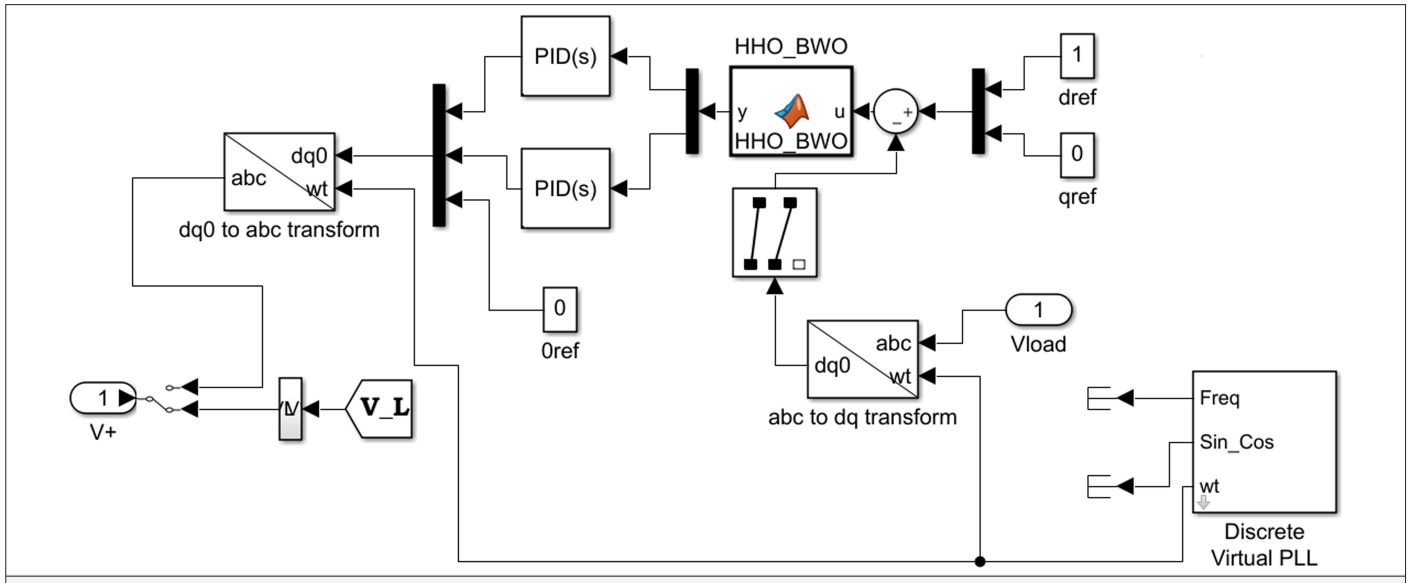

Fig. 5. Simulink diagram of the proposed work.

supply (Fig. 7). As an injected voltage is injected into the load voltage, the Z-DVR also produced a small amount of voltage harmonics signal (Fig. 7). This voltage is injected as a result of the harmonic voltage drop in the filter. The RMS of the source signal with the same period fault and corrected load voltage is also shown in clear detail in Fig. 7. The proposed HHO–BWO controlled the Z-DVR model to account for the degree of voltage concerns.

A. Case 1: Voltage Sag Compensation With ZSI-DVR

Figure 8 shows the simulation results of the sag's grid voltage, RMS voltage of the grid, injection voltage, and load voltage. In the supply side voltage, 20% of the sag occurs on the voltage, which is the sag voltage that begins from 0.15 seconds to 0.35 seconds. To inject the compensating voltage to normalize the sag voltage and maintain the stable voltage, the ZSI-DVR is connected to the system for some time of 0.15 seconds to 0.35 seconds.

1) Comparison of Sag Voltage With ZSI-DVR

While using the proposed HHO–BWO–PID with Z-DVR, the output voltage demonstrates superiority over the conventional methods such as BWO–PID, HHO–PID, and GA–PID controllers during the 3-φ fault. The output voltage shows that the suggested HHO–BWO–PID with Z-DVR is superior to the traditional approaches, such as BWO–PID, HHO–PID, and GA–PID controllers, during the 3-φ fault. The comparison of the suggested sag voltage compensation with the established techniques is shown in Fig. 9.

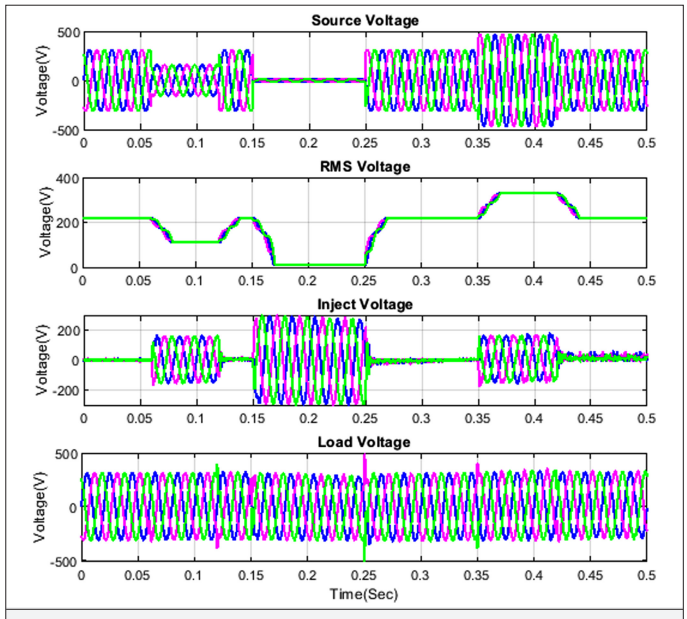

Fig. 6. Simulink diagram of the control structure of the proposed HHO–BWO. BWO, black widow optimization; HHO, Harris hawks optimization.

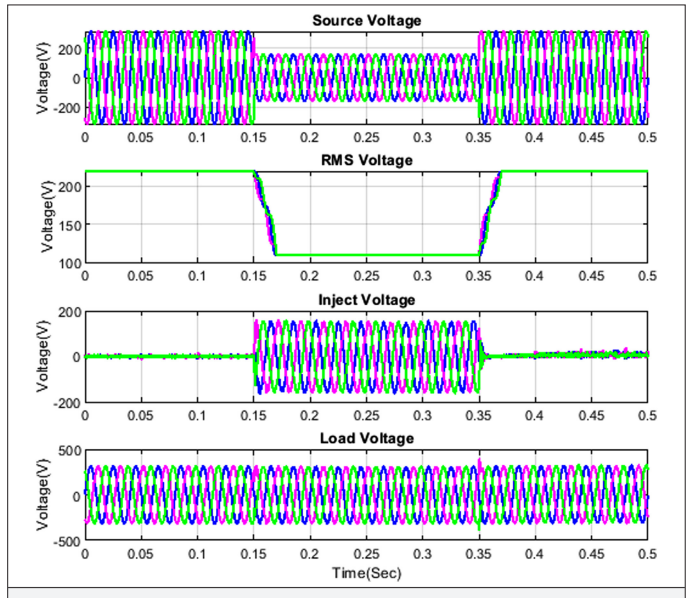

Fig. 7. Simulation outcomes of fault signal, RMS, compensating signal, and load voltage without fluctuation. RMS, root mean square.

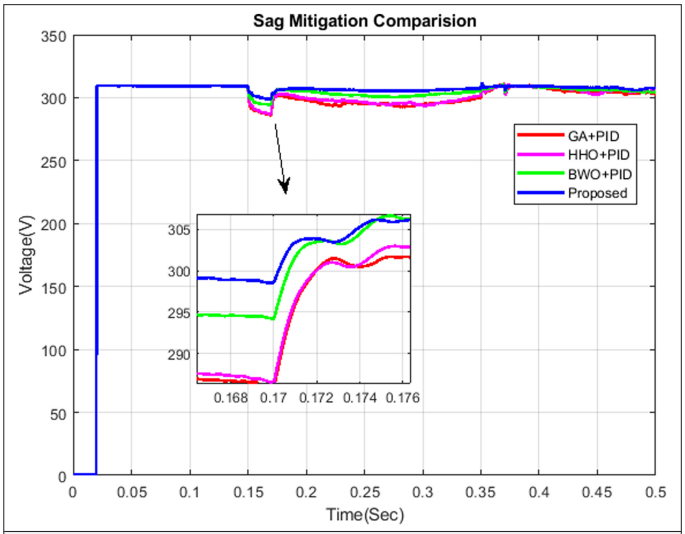

Fig. 8. Simulation results of sag's grid voltage, RMS voltage of grid, injection voltage, and load voltage. RMS, root mean square.

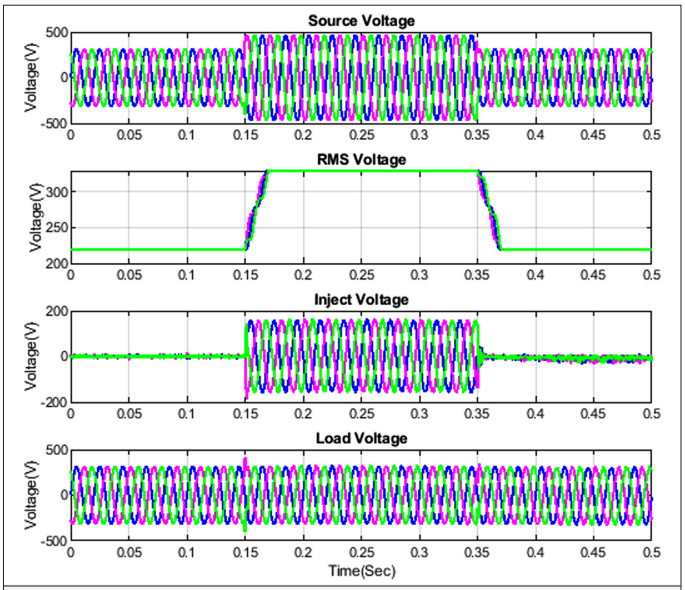

Fig. 9. Comparison of the sag compensation.

B. Case 2: Voltage Swell Compensation With ZSI-DVR

The performance of the suggested technique is predicted using the swell condition. By fusing the problem and the source, the swell condition is introduced into the system. When examining the swell state, a variety of sources are used, and performances are evaluated. Fig. 10 demonstrates how the mitigated voltage swell signal was assessed using Z-DVR. The fault in this instance occurs within the range of 0.15 seconds to 0.35 seconds, overshooting the swell signal. A compensated load voltage of 320 V is produced by using the Z-DVR to adjust the swell signal with the injected voltage.

1) Swell Comparison With ZSI-DVR

During the 3-φ fault, the output voltage of the proposed HHO–BWO–PID with Z-DVR is superior to that of traditional approaches such as BWO–PID, HHO–PID, and GA–PID controllers. The proposed

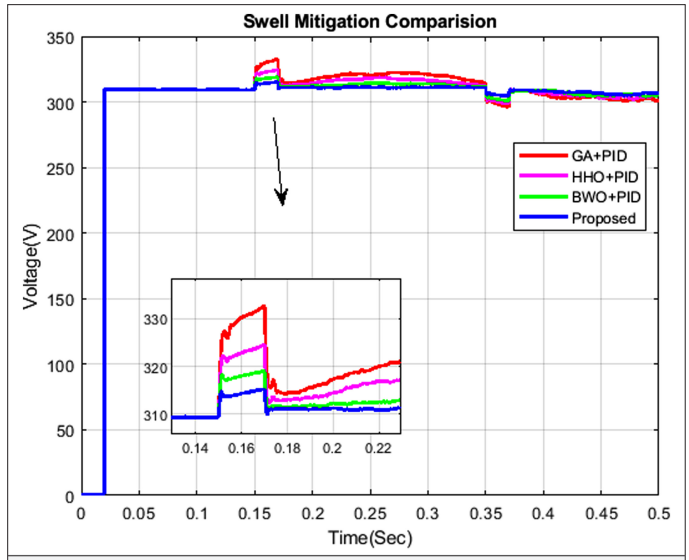

Fig. 10. Simulation results of Swell's grid voltage, RMS voltage of grid, injection voltage, and load voltage. RMS, root mean square.

sag voltage compensation method is compared to the standard approaches in Fig. 4.

C. Case 3: Voltage Fluctuation Compensation With ZSI-DVR

Figure 11 illustrates the 3-φ fault application between 0.15 seconds and 0.35 seconds for supply fluctuation analysis of the Z-DVR's implementation of voltage compensation. It also shows a very little amount of the voltage harmonics signal that the Z-DVR produced as it injected voltage into the load voltage. The filter's harmonic voltage drop is what causes this injected voltage to happen. Additionally, it explains the RMS of the source signal with the identical period fault

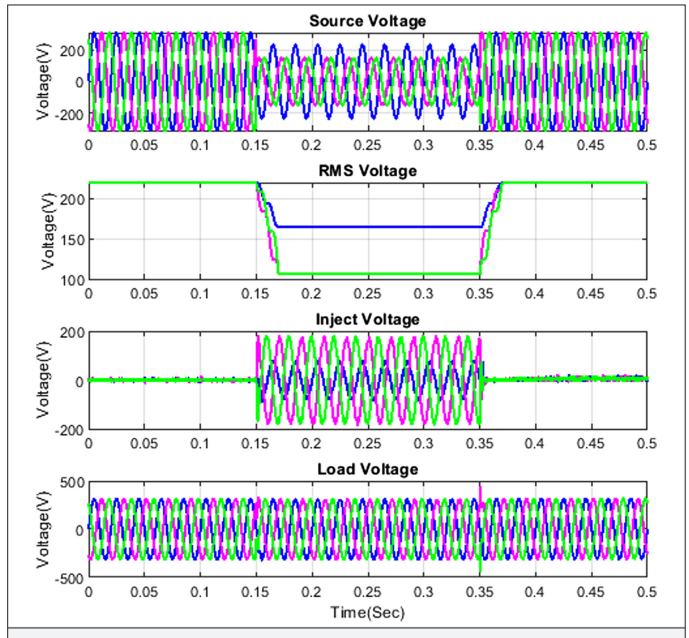

Fig. 11. Simulation results of fluctuation of grid voltage, RMS voltage of grid, injection voltage, and load voltage. RMS, root mean square.

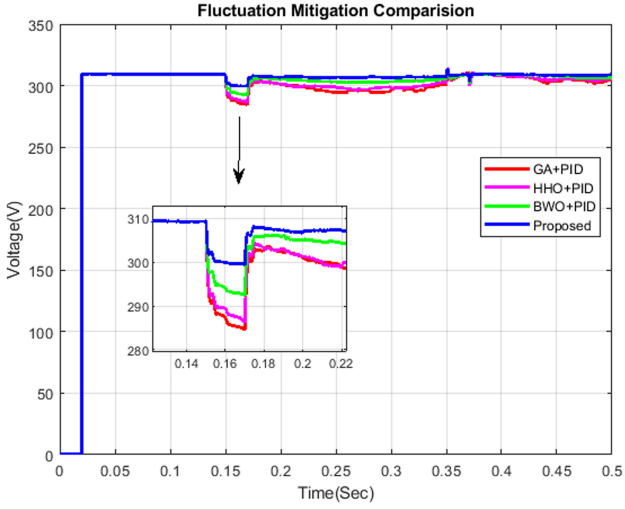

Fig. 12. Comparison of the fluctuation compensation.

and corrected load voltage. The Z-DVR model was regulated by the proposed HHO–BWO to account for the severity of the voltage problems.

1) Fluctuation Comparison With ZSI-DVR

Comparing the correction of fluctuation to traditional optimization methods such as BWO with PID, HHO with PID controller, and GA with PID controller is shown in Fig. 12. The planned voltage reached 320 V, and between 0.15 seconds and 0.35 seconds later, a fault developed on the source voltage. To maintain a stable load voltage at such time, the Z-DVR applied an injected voltage through a transformer to the fluctuating voltage. The proposed Z-DVR is superior to the other standard controller (Fig. 12).

D. Case 4: Voltage Interruption Compensation With ZSI-DVR

The simulation results for the interrupted grid voltage, the grid voltage's RMS voltage, the injected voltage, and the load voltage are shown in Fig. 13. To assess the implementation of the Z-DVR for

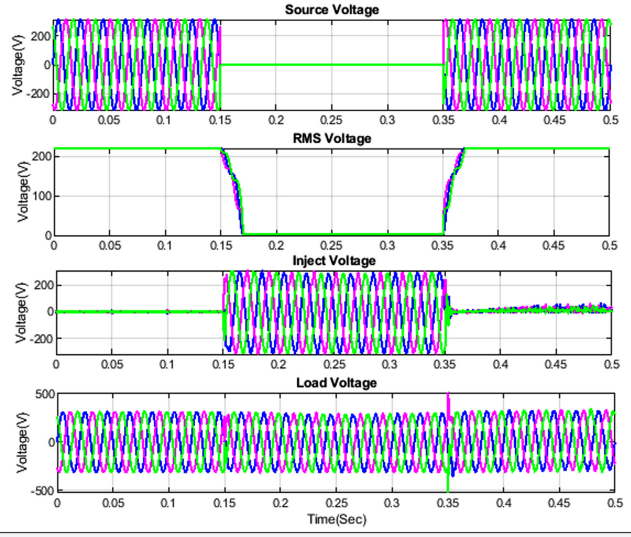

Fig. 13. Simulation results of interruption' grid voltage, RMS voltage of grid, injection voltage, and load voltage. RMS, root mean square.

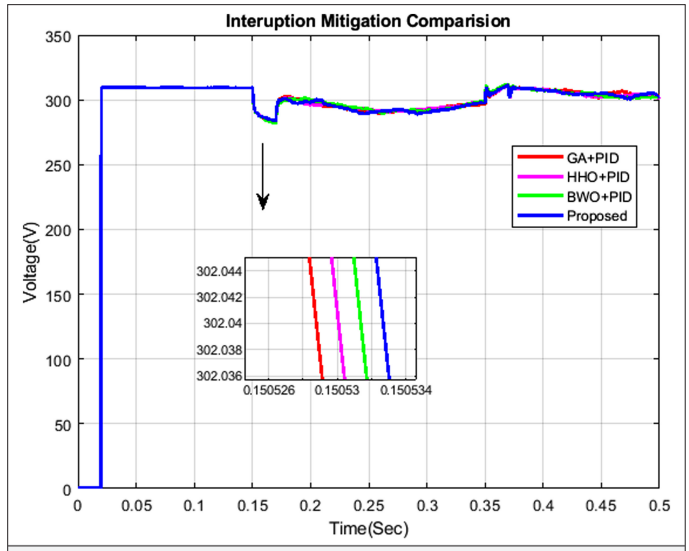

Fig. 14. Comparison of the interruption compensation.

voltage compensation, the 3-φ fault is applied between the time length of 0.15 seconds and 0.35 seconds. It also shows a very little amount of the voltage harmonics signal that the Z-DVR generated while injecting a voltage into the load voltage. This injected voltage occurs due to the filter's harmonic voltage drop. RMS of the source signal with the same duration fault and compensated load voltage is also clearly clarified in Fig. 13. The proposed HHO–BWO controlled the Z-DVR model to compensate for the magnitude of the voltage issues.

1) Interruption Comparison With ZSI-DVR

When compared to traditional optimization methods like BWO with PID, HHO with PID controller, and GA with PID controller, the compensation of interruption is shown in Fig. 14. The planned voltage reached 320 V, and between 0.15 seconds and 0.35 seconds later, a fault developed on the source voltage. To maintain a stable load voltage at that time, the Z-DVR injects the injected voltage into the interrupted voltage through the transformer. The proposed Z-DVR is superior to the other standard controller (Fig. 14).

E. THD Estimation

Figure 15 compares the THD of the proposed methodology HHO–BWO with the Z-DVR technique to that of more traditional methods like BWO–PID, HHO–PID, and GA–PID. In this diagram, the harmonic mitigation is shown as 1.06% for the HHO–PID, 1.01% for the BWO–PID, and 0.87% for the HHO–BWO–PID controller concerning frequency in Hertz. The suggested methodology, which makes use of Z-DVR-based improved HHO–BWO–PID controller techniques, is effective at mitigating voltage quality difficulties.

The comparison of the THD percentage with traditional approaches is shown in Table II. The THD percentage for the mm-sized resistance-typed sensor film (MRSF) controller is 2.99%, the percentage for the GA-based PID controller is 1.18%, the percentage for the HHO-based PID controller is 1.06%, and the percentage for the BWO–PID is clearly showing that the suggested technique is more accurate than the existing techniques.

As demonstrated in this result section, the suggested Z-DVR with an HHO–BWO-based PID controller considerably reduces voltage issues

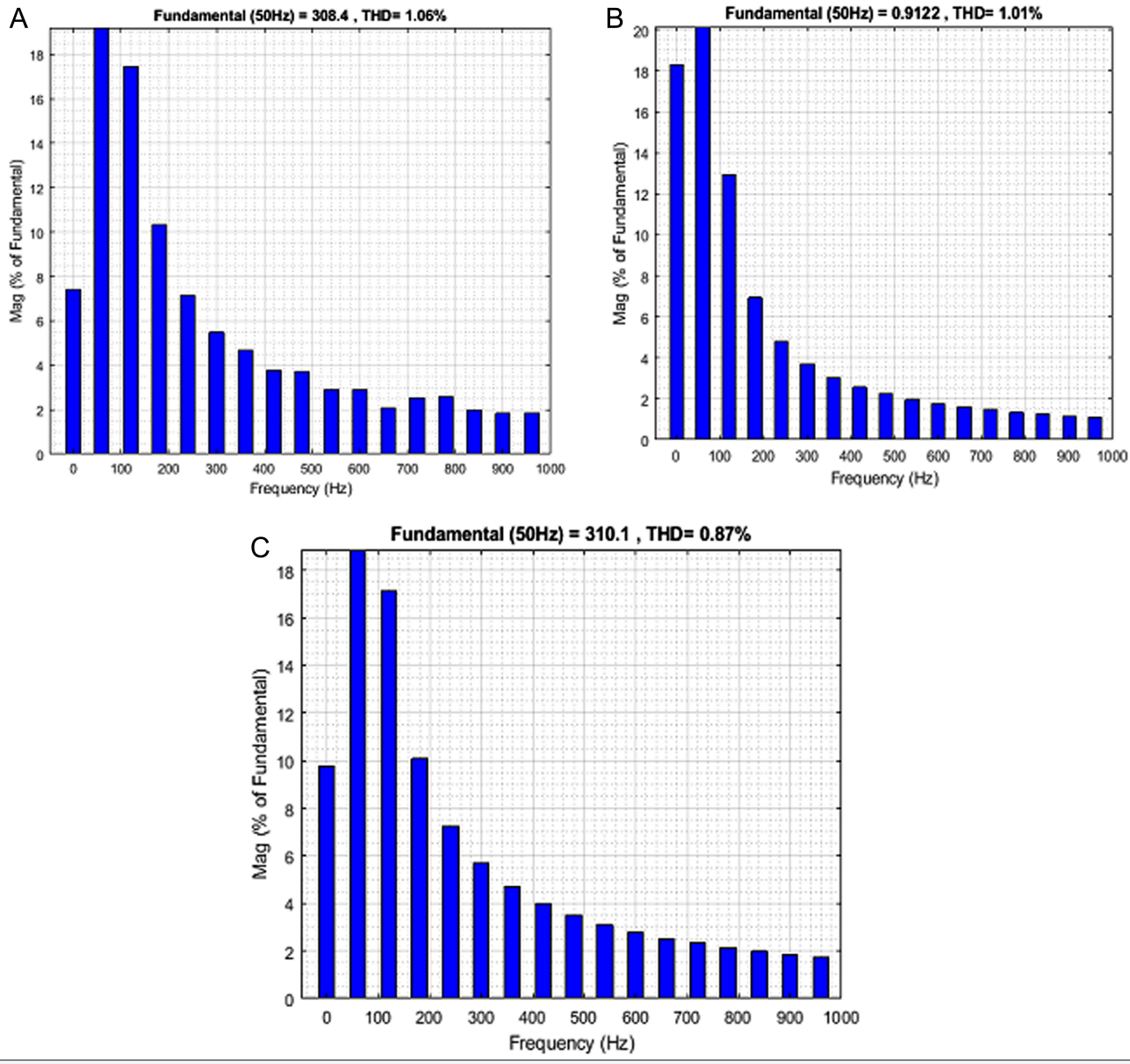

Fig. 15. THD % of proposed and conventional techniques (A) HHO–PID, (B) BWO–PID, and (C) HHO–BWO–PID. BWO, black widow optimization; HHO, Harris hawks optimization; PID, proportional–integral–derivative controller; THD, total harmonic distribution.

TABLE II. THD % WITH CONVENTIONAL TECHNIQUE

Methods	THD %
MRSF controller with Z-DVR	2.99%
GA–PID controller with Z-DVR	1.18%
HHO–PID with Z-DVR	1.06%
BWO–PID with Z-DVR	1.01%
HHO–BWO–PID with Z-DVR	0.87%

BWO, black widow optimization; GA, genetic algorithm; HHO, Harris hawks optimization; MRSF, mm-sized resistance-typed sensor film; PID, proportional–integral–derivative controller; THD, total harmonic distribution; Z-DVR, Z-source dynamic voltage restorer;

when compared to conventional controllers like BWO-based PID controller, HHO-based PID controller, GA-based PID controller, and MRSF controller.

VI. CONCLUSION

A smart and effective compensatory mechanism based on Z-DVR is suggested as a solution to the power distribution system's voltage problems. To address these issues, the proposed HHO–BWO with PID-controlled Z-DVR has been demonstrated under non-linear load conditions. These issues include harmonics, sag, fluctuation, swell, and interruption. According to the results of the simulation that was run, Z-DVR can correct all-power problems and shield sensitive loads from source-side disturbances. Additionally, Z-DVR preserved the supplied reference value under balanced and unbalanced conditions with no additional disturbances to reduce those voltage

problems and correct the load voltage at the lowest value by injecting the right voltage component. The proposed Z-DVR model was also created in MATLAB/Simulink. The suggested HHO–BWO with PID offers more effective compensation than the earlier works, as well as an inexpensive DVR device, has a quick dynamic reaction, and is small in size.

Peer-review: Externally peer-reviewed.

Author Contributions: Concept – C.S.K., Z.M.L.; Design – C.S.K.; Supervision – Z.M.L.; Funding – No Funding; Materials – C.S.K., Z.M.L.; Data Collection and/or Processing – C.S.K., Z.M.L.; Analysis and/or Interpretation – C.S.K.; Literature Review – C.S.K.; Writing – C.S.K.; Critical Review – Z.M.L.

Declaration of Interests: The authors declare that they have no competing interest.

Funding: The authors declared that this study has received no financial support.

REFERENCES

1. M. Bajaj, A. K. Singh, M. Alowaidi, N. K. Sharma, S. K. Sharma, and S. Mishra, "Power quality assessment of distorted distribution networks incorporating renewable distributed generation systems based on the analytic hierarchy process," *IEEE Access*, vol. 8, pp. 145713–145737, 2020. [CrossRef]
2. A. Moreno-Munoz, J. J. G. de-la-Rosa, M. A. Lopez-Rodriguez, J. M. Flores-Arias, F. J. Bellido-Outerino, and M. Ruiz-de-Adana, "Improvement of power quality using distributed generation," *Int. J. Elect. Power Energy Syst.*, vol. 32, no. 10, pp. 1069–1076, 2010. [CrossRef]
3. J. O. Petinrin and M. Shaabanb, "Impact of renewable generation on voltage control in distribution systems," *Renew. Sustain. Energy Rev.*, vol. 65, pp. 770–783, 2016. [CrossRef]
4. C. Muscas, "Power quality monitoring in modern electric distribution systems," *IEEE Instrum. Meas. Mag.*, vol. 13, no. 5, pp. 19–27, 2010. [CrossRef]
5. H. Abdollahzadeh, M. Jazaeri, and A. Tavighi, "A new fast-converged estimation approach for dynamic voltage restorer (DVR) to compensate voltage sags in waveform distortion conditions," *Energy Syst.*, vol. 54, pp. 598–609, 2014. [CrossRef]
6. H. Liao and J. V. Milanović, "On capability of different FACTS devices to mitigate a range of power quality phenomena," *IET Gener. Transm. & Distrib.*, vol. 11, no. 5, pp. 1202–1211, 2017. [CrossRef]
7. E. Hossain, M. R. Tur, S. Padmanaban, S. Ay, and I. Khan, "Analysis and mitigation of power quality issues in distributed generation systems using custom power devices," *IEEE Access*, vol. 6, pp. 16816–16833, 2018. [CrossRef]
8. A. Amita and A. K. Sinha, "Power quality comparison of grid connected wind energy system with STATCOM and UPQC," International Conference on Intelligent Circuits and Systems (ICICS), 2018. [CrossRef]
9. V. Ansal, "ALO-optimized artificial neural network-controlled dynamic voltage restorer for compensation of voltage issues in distribution system," *Soft Comput.*, vol. 24, no. 2, pp. 1171–1184, 2020. [CrossRef]
10. R. Pal, and S. Gupta, "Topologies and control strategies implicated in dynamic voltage restorer (DVR) for power quality improvement," *Iran. J. Sci. Technol. Trans. Electr. Eng.*, vol. 44, no. 2, pp. 581–603, 2020. [CrossRef]
11. M. M. Ghahderijani, M. Castilla, L. G. de Vicuna, A. Camacho, and J. T. Martinez, "Voltage sag mitigation in a PV-based industrial microgrid during grid faults," 2017 IEEE 26th International Symposium on Industrial Electronics (ISIE). IEEE Publications, 2017. [CrossRef]
12. A. B. Kunya, T. Yalcinoz, and G. S. Shehu, "Voltage sag and swell alleviation in distribution network using custom power devices; D-STATCOM and DVR," 2014 16th International Power Electronics and Motion Control. Conference and Exposition. 2014. [CrossRef]
13. M. Balamurugan, T. S. Sivakumaran, and M. Aishwariya, "Voltage sag/swell compensation using Z-source inverter DVR based on FUZZY controller," 2013 IEEE International Conference ON Emerging Trends in Computing, Communication and Nanotechnology (ICECCN). 2013. [CrossRef]
14. C. E. Thenmozhi, C. Gopinath, and R. Rames, "A novel method for voltage sag/swell compensation using Dynamic Voltage Restorer," in IEEE-International Conference on Advances in Engineering, Science and Management (ICAESM-2012). IEEE Publications, 2012, pp. 333–338.
15. Y. Xu, L. M. Tolbert, J. D. Kueck, and D. T. Rizy, "Voltage and current unbalance compensation using a static var compensator," *IET Power Electron.*, vol. 3, no. 6, p. 977, 2010. [CrossRef]
16. E. A. Al-Ammar, A. Ul-Haq, A. Iqbal, M. Jalal, and A. Anjum, "SRF based versatile control technique for DVR to mitigate voltage sag problem in distribution system," *Ain Shams Eng. J.*, vol. 11, no. 1, pp. 99–108, Mar. 2020. [CrossRef]
17. B. S. Joshi, O. P. Mahela, and S. R. Ola, "Reactive power flow control using Static VAR Compensator to improve voltage stability in transmission system," 2016 International Conference on Recent Advances and Innovations in Engineering (ICRAIE). 2016. [CrossRef]
18. F. B. Moreno, J. E. Palacios, J. Posada, and J. A. Lopez, "Implementation and evaluation of a new DVR topology with AC link for series compensation," *Electr. Power Syst. Res.*, vol. 181, p. 106184, Apr. 2020. [CrossRef]
19. S. V. Bhonde, S. S. Jadhao, and R. S. Pote, "Enhancement of voltage quality in power system through series compensation using DVR," International Conference on Current Trends in Computer, Electrical, Electronics and Communication (CTCEEC). 2017. [CrossRef]
20. P. K. Ray, S. R. Das, and A. Mohanty, "Fuzzy-controller-designed-PV-based custom power device for power quality enhancement," *IEEE Trans. Energy Convers.*, vol. 34, no. 1, pp. 405–414, Mar. 2019. [CrossRef]
21. E. M. Molla and C.-C. Kuo, "Voltage sag enhancement of grid connected hybrid PV-wind power system using battery and SMES based dynamic voltage restorer," *IEEE Access*, vol. 8, pp. 130003–130013, 2020. [CrossRef]
22. D. Rajasekaran, S. S. Dash, and P. Vignesh, "Mitigation of voltage sags and voltage swells by dynamic voltage restorer," 3rd International Conference on Advances in Recent Technologies in Communication and Computing (ARTCom 2011). 2011. [CrossRef]
23. E. Babaei, F. M. Shahir, S. D. Tabrizi, and M. Sabahi, "Compensation of voltage sags and swells using photovoltaic source based DVR," 2017 14th International Conference on Electrical Engineering/Electronics, Computer, Telecommunications and Information Technology (ECTI-CON). 2017. [CrossRef]
24. C. K. Sundarabalan and K. Selvi, "Compensation of voltage disturbances using PEMFC supported Dynamic Voltage restorer," *Energy Syst.*, vol. 71, pp. 77–92, 2015. [CrossRef]
25. D. A. Ingole, and P. D. V. N. Gohokar, "Voltage Stability Improvement In Multi-bus System Using Static Synchronous Series Compensator" *Energy Procedia*, vol. 117, pp. 999–1006, 2017. [CrossRef]
26. C. Kumar, P. Ghosh, and S. Chatterjee, "Enhancement of Power Quality by mitigating of sag and swell problem in power system using DVR," *IFAC PapersOnLine*, vol. 55, no. 1, pp.131–137, 2022. [CrossRef]
27. S. Shirke and S. S. Khule, "Improved DC bus utilization of DVR based on repetitive controller with THIPWM technique," *Glob. Transit. Proc.*, vol. 3, no. 1, pp.257–266, 2022. [CrossRef]
28. D. Prasad and C. Dhanamjayulu, "Solar PV integrated dynamic voltage restorer for enhancing the power quality under distorted grid conditions," *Electr. Power Syst. Res.*, vol. 213, p.108746, 2022. [CrossRef]

Ch Srivardhan Kumar is an engineering graduate. He has completed (B.Tech) Electrical and Electronics Engineering from JNTU Hyderabad, Telangana. He has done his Master's in Power Electronics from JNTU Hyderabad. Currently, he is pursuing Ph.D. in Sathyabama Institute of Science and Technology, Chennai. His research area is Power Electronics application in power system. He has published seven papers in various international journals.

Z. Mary Livinsa is currently working as Associate Professor in Sathyabama Institute of Technology, Chennai. She is an Engineering graduate in Electronics and Communication Engineering, from Noorul Islam College of Engineering, Nagercoil. She did her master's from Sathyabama University, Chennai and Ph.D. in Sathyabama Institute of Science and Technology, Chennai. Her research area is wireless sensor network, and area of interest is power electronics application in power system and wireless network. She has published over 20 papers in national and international journals.